

## Cell Biosensors: Rapid Detection and Identification of Pathogens Using FTIR Microspectroscopic Spectra

**Drs. Julia Hilliard, Chadi Filfili, Irina Patrusheva, Pinhas Fuchs, and David Katz**

Viral Immunology Center, Department of Biology  
Georgia State University  
Atlanta, GA 30302  
USA

(404) 413-6560 / fax (404) 413-6561

[jhilliard@gsu.edu](mailto:jhilliard@gsu.edu)

**Drs. Ruili Wang, Gary Hastings and Ms. Jing Guo**

Department of Physics and Astronomy  
Georgia State University  
P.O. Box 4118  
Atlanta, GA 30302  
USA

**Yu-Sheng Hsu**

Department of Mathematics  
Georgia State University  
P.O. Box 4118  
Atlanta, GA 30302  
USA

**John Ward, Ph.D.**

Department of Clinical Investigation  
Brooke Army Medical Center  
Fort Sam Houston, San Antonio, TX  
USA

### **ABSTRACT**

*Life threatening virus infections require the earliest possible identification in order to save lives and preserve wellbeing. Field detection of viruses causing infection is vital to limit the detrimental effects of pathogen spread. Currently, rapid identification of specific virus infections requires a minimum of days-to-weeks to accomplish, often requiring expansion of virus in cell culture before application of other diagnostic techniques, e.g., PCR, which requires some knowledge of what type of virus is involved for selection of appropriate primers, or immunoassays.*

*We hypothesized that cells can be utilized as biosensors that can be probed using FTIR microspectroscopy to identify specific viruses to which they are exposed. We envision that this technology can be contained within a portable device to probe for infectious virus. To test this hypothesis, we exposed cells to virus or mock-infected cell lysates to determine the earliest time points at which virus could be detected, identified, and differentiated from other agents. Next, spectral bands that discriminated between viruses were selected and a neural network was trained to classify the spectra based on the selected bands. Finally, we identified specific intracellular signaling pathways in cells at different time points following exposure to selected viruses. Induction of specific signaling pathways initiates the innate defenses in the cell in response to specific viruses. Each specific virus has evolved and selected for different strategies to redirect these innate defenses to permit the virus to replicate successfully, a process, which is dependent on the cell remaining viable.*

---

Disclaimer: The opinions or assertions herein are the private views of the authors and are not to be construed as reflecting the views of the Department of the Army or the Department of Defense.

## Report Documentation Page

Form Approved  
OMB No. 0704-0188

Public reporting burden for the collection of information is estimated to average 1 hour per response, including the time for reviewing instructions, searching existing data sources, gathering and maintaining the data needed, and completing and reviewing the collection of information. Send comments regarding this burden estimate or any other aspect of this collection of information, including suggestions for reducing this burden, to Washington Headquarters Services, Directorate for Information Operations and Reports, 1215 Jefferson Davis Highway, Suite 1204, Arlington VA 22202-4302. Respondents should be aware that notwithstanding any other provision of law, no person shall be subject to a penalty for failing to comply with a collection of information if it does not display a currently valid OMB control number.

1. REPORT DATE

**APR 2010**

2. REPORT TYPE

**N/A**

3. DATES COVERED

-

4. TITLE AND SUBTITLE

**Cell Biosensors: Rapid Detection and Identification of Pathogens Using FTIR Microspectroscopic Spectra**

5a. CONTRACT NUMBER

5b. GRANT NUMBER

5c. PROGRAM ELEMENT NUMBER

6. AUTHOR(S)

5d. PROJECT NUMBER

5e. TASK NUMBER

5f. WORK UNIT NUMBER

7. PERFORMING ORGANIZATION NAME(S) AND ADDRESS(ES)

**Viral Immunology Center, Department of Biology Georgia State University Atlanta, GA 30302 USA**

8. PERFORMING ORGANIZATION REPORT NUMBER

9. SPONSORING/MONITORING AGENCY NAME(S) AND ADDRESS(ES)

10. SPONSOR/MONITOR'S ACRONYM(S)

11. SPONSOR/MONITOR'S REPORT NUMBER(S)

12. DISTRIBUTION/AVAILABILITY STATEMENT

**Approved for public release, distribution unlimited**

13. SUPPLEMENTARY NOTES

**See also ADA564622. Use of Advanced Technologies and New Procedures in Medical Field Operations (Utilisation de technologies avancees et de procedures nouvelles dans les operations sanitaires). RTO-MP-HFM-182**

14. ABSTRACT

**Life threatening virus infections require the earliest possible identification in order to save lives and preserve wellbeing. Field detection of viruses causing infection is vital to limit the detrimental effects of pathogen spread. Currently, rapid identification of specific virus infections requires a minimum of days-to-weeks to accomplish, often requiring expansion of virus in cell culture before application of other diagnostic techniques, e.g., PCR, which requires some knowledge of what type of virus is involved for selection of appropriate primers, or immunoassays. We hypothesized that cells can be utilized as biosensors that can be probed using FTIR microspectroscopy to identify specific viruses to which they are exposed. We envision that this technology can be contained within a portable device to probe for infectious virus. To test this hypothesis, we exposed cells to virus or mock-infected cell lysates to determine the earliest time points at which virus could be detected, identified, and differentiated from other agents. Next, spectral bands that discriminated between viruses were selected and a neural network was trained to classify the spectra based on the selected bands. Finally, we identified specific intracellular signaling pathways in cells at different time points following exposure to selected viruses. Induction of specific signaling pathways initiates the innate defenses in the cell in response to specific viruses. Each specific virus has evolved and selected for different strategies to redirect these innate defenses to permit the virus to replicate successfully, a process, which is dependent on the cell remaining viable.**

15. SUBJECT TERMS

16. SECURITY CLASSIFICATION OF:			17. LIMITATION OF ABSTRACT <b>SAR</b>	18. NUMBER OF PAGES <b>12</b>	19a. NAME OF RESPONSIBLE PERSON
a. REPORT <b>unclassified</b>	b. ABSTRACT <b>unclassified</b>	c. THIS PAGE <b>unclassified</b>			

**Standard Form 298 (Rev. 8-98)**  
Prescribed by ANSI Std Z39-18

## **INTRODUCTION**

The identification of agents that cause infection is often a labor-intensive process often requiring relatively sophisticated laboratories and highly trained personnel. Days to weeks can be required before laboratory staff can inform medical personnel of the identity of an infectious agent. More rapid identification requires some knowledge about the likely identity of the etiologic agent, e.g., outbreaks of influenza where many share common symptoms around the same time period. Most of the time, however, considerable time lapses before unequivocal identification of infectious agents can be accomplished, delaying effective pharmacologic intervention and slowing the process of intervention by medical personnel.

Among the most frequent causes of infectious disease are viruses. Viruses often must be grown in cell cultures for days to weeks before significant concentrations of these are available for identification. Even after expansion of virus isolates in culture, the identification of the virus requires considerable expertise. Antibodies that react with the virus isolates can be used to perform immuno-fluorescence assays (IFA) or enzyme immunoassays (ELISA), however, in the absence of some knowledge about the identity of the virus, it is not possible to know which antibodies to use. The same holds true with using polymerase chain reaction (PCR), a technique, which may save considerable time and avoid the time loss due to trying to expand virus in cell culture. Without some foreknowledge it is not possible to select primers to amplify viral DNA or RNA. Each of these methods depends on the success of collecting specimens that contain the virus responsible for the infection under investigation. Identification of the etiologic agent is the gold standard for diagnosis of infectious diseases, yet in many infections, isolation of the causative agent is not successful. For this reason, indirect detection of infectious agents is often the only way to identify pathogens. These detection strategies rely on detection of host responses induced by the presence of the pathologic agent, e.g., induction of antibodies, biomarkers, or other secondary indicators. Antibodies are most often the target for detection to identify the causative agent, but these take the host 7-14 days or sometimes considerably longer to produce in concentrations sufficient for detection. Furthermore, paired samples collected at two different time points at least 14-21 days apart are required to validate that the specific antibodies are increasing and are not simply present from an earlier, unrelated infection. The other caveat is that again some knowledge of the suspect agent is needed to capture the antibodies, a process that requires use of homologous or heterologous virus responsible for the infection and immunoreactive with the induced serum antibodies. The challenges of direct and indirect detection strategies currently available clearly make identification of infectious diseases time consuming, expensive endeavors.

The most sophisticated and sensitive sensors of infectious diseases are cells exposed to the etiologic agents [1,2,3]. Cells respond immediately to viruses, bacteria, fungi, and parasites in unique ways. Cells encountering an agent immediately set off multiple defense alarms. For example, cells respond differently to each type of virus encountered as a result of the types of receptors engaged on the cell surface as well as within the cells. Cell responses are further defined by the virus-specific interruption of selected defense pathways, so two very similar viruses that engage the same receptor on the cell surface may have distinctly different abilities to effect intracellular signaling. Differences in the types of cell defenses, the specificities of virus interference, and the kinetics of induction of cell pathways all work together and can be exploited to define the pathogen encountering cells. Amazingly, these processes are put into motion within minutes to hours after the cell: pathogen encounter. Detection of the interplay of cell sensing and pathogen presence, however, also requires considerable time and effort. Therefore, we hypothesized that infrared microscopic interrogation of cells exposed to pathogenic viruses results in spectral profiles that can be used to identify specific pathogens within hours after exposure of cells in culture to virus-containing specimens. Although, considerable technology is required for virus detection and identification using this approach, we conceived the idea that proof of this concept could lead to the design of a portable field device that would obviate the

need for sophisticated clinical laboratories, trained staff, and time required currently for pathogen identification.

## MATERIALS AND METHODS

### Cells and Virus

We selected Vero cells in culture to serve as biosensors of infection because these cells do not produce interferon, and thus are permissive to a broad range of viruses. Vero cells (ATCC, CCL 81) were grown and passaged in Dulbecco's modified Eagles media containing 10% heat inactivated fetal calf serum, penicillin (100 U/ml), and streptomycin (100 µg/ml). We selected three different viruses for the proof-of-concept experiments presented here, herpes simplex virus type 1 (F strain) (HSV-1), coxsackie virus B3 (CX), and human adenovirus type 5 (Ad5). Each virus stock was obtained from ATCC and subsequently propagated on Vero cells, as needed, to produce single stock viruses for use in each experiment. We prepared virus stocks from infected cells by freeze-thawing these at 48 hours post infection. Each virus stock was quantified using the standard plaque assay to enable us to equalize infectious virus particles to be used to define each virus-specific infected cell infrared spectrum. Vero cells were infected at 90-95% confluency in log phase growth using a multiplicity of infection (MOI) of 10 to ensure that each cell in the monolayer was infected, establishing that each cell would be responding similarly in order to define the cell spectrum when a specific virus was encountered. The control for each cell sensor was exposure to uninfected, lysed Vero cells (Mock infections) prepared in an identical manner to virus stock as described above. Infected and mock infected cells were harvested at various time points following infection, including two hours, four hours, six hours, and 24 hours. Cells were harvested by scraping into PBS using a plastic cell scraper, then pelleted, and resuspended in PBS for application to ZnSe or Low E windows for analysis. Infections presented in this paper were repeated 20 times to permit statistical processing of data to determine the sensitivity and specificity of the spectra generated by each virus infected cell sample and to allow for sufficient numbers of samples to train the locally developed neural network for analysis of automated processing.

### Analysis of Cells Using FTIR Microspectroscopy

Virus or mock-infected cells placed onto ZnSe windows were air dried and subsequently examined within 30 minutes. FTIR measurements were made using a Varian 7000 FTIR spectrometer that is coupled to a Varian UMA600 IR microscope (Stingray system). The microscope has both IR transmission and reflection capabilities, using on-axis, matched 15 X Schwartzchild objectives and condenser. The microscope is also equipped with a visible light source and a visible 640 X 480 CCD camera, which allows capture of visible microscopic images from the same region that is interrogated via FTIR. Analysis was performed at 2 cm<sup>-1</sup> resolution. [4,5]

### Data Processing

Spectra were imported into an Excel Spreadsheet to perform vector normalization and offset correction using OPUS software. We calculated the 21-point moving minimum from the vector normalized and offset corrected data for each spectrum. We compared the normalized waveform to its 21-point moving minimum. If the difference was less than a threshold value, at any given wavenumber, we selected that wavenumber as a potential critical point. We selected those critical points that were common to a minimum number of spectra. The threshold value and minimum number of spectra were selected by observing the number and location of critical points on a graph of the average normalized spectrum. We selected the wavenumbers 799, 892, 941,

1185, 1290, 1349, 1427, 1479, and 1492  $\text{cm}^{-1}$  as critical wavenumbers. We calculated the slope and intercept of the straight lines between the absorbance at each of those points and stored the results in a lookup table. We calculated a piecewise linear baseline from the values in the lookup table. We subtracted the piecewise linear baseline from the normalized spectrum. We selected three representative waveforms to illustrate the results of piecewise linear baseline subtraction.

## **Statistical**

A pairwise comparison method was used to minimize Fourier transform infrared spectroscopy data variability among intra-group experiments. To accomplish this, pairwise comparison of inter-group values such as virus infected versus mock infected cells from multiple experiments performed over a one year period were performed. We standardized and smoothed the spectra following FTIR analyses, then used the Wilcoxon-rank-sum test with Bonferroni's correction to select the frequency ranges that may optimally differentiate viruses. Finally, we used either logistic regression or the partial least squares method to find spectral markers by which we can differentiate these viruses. To gauge the goodness of the spectral markers, we used sensitivity, specificity, and area under the receiver-operating-characteristic (ROC) curve to measure the discriminating power. A straightforward principal-components method and a simple t-test have been commonly used also, but sensitivity, specificity, and area under ROC curves performed superior to the other tests. We also used cross-validation as well as bootstrap methods to compare the shrinkages of the above measurements.

## **Neural Network Analysis of Processed Data**

Spectra from Vero cells exposed to mock, HSV 1, adenovirus, and coxsackie virus were standardized within infections by normalizing individual spectra to mean and standard deviation, smoothing with a five-point moving average and averaging twenty spectra from each of 20 datasets by 3 infections by 3 times, which equals 180 observations. Graphical and ROC curve analysis were used to select discriminators. Ten discriminators consisting of absorption and difference spectra from bands centered at 1086 and 1301  $\text{cm}^{-1}$  were used to train a 10 X 12 X 3 feed forward, back propagation neural network with 10 data sets and test it with 10 data sets.

## **Parallel Analysis of Temporal Molecular Events in the Cell Biosensor**

We used the Human Proteome Profiler Arrays to identify the specificity and kinetics of signal transduction pathways that were induced following exposure of the Vero cell biosensors in culture. We also performed real-time polymerase chain reaction (RT-PCR) microarray studies at selected time-points of infection using HSV-1, human adenovirus type 5 (Ad5), and CX. The first array detected the genes that express chemokines, cytokines, and their receptors (PAHS-011, SuperArray Bioscience) that provide insight into the cell biosensors' defenses that are not disrupted by virus-specific proteins. The second array (PAHS-014, SuperArray Bioscience) profiled the expression of key genes related to the signal transduction cascades. The third array profiled the expression of key genes related to the induction of NF $\kappa$ B-mediated signal transduction pathways (PAHS-025, SuperArray Bioscience). SuperArray Bioscience web-based software was used to compare the expression data from virus- and mock-infected cell biosensors at two, four, eight, 12, and 24 hours following exposure of cells to infected and uninfected cell lysates. For each array experiment, total RNA was prepared from the virus- and mock-infected cells using the RNeasy Miniprep protocol (Qiagen) and used to generate cDNA for quantitative real-time PCR (qPCR). An aliquot of 3.5  $\mu\text{g}$  of RNA from each sample was converted to cDNA using RT2 First Strand Kit (C-03; SuperArray Bioscience). Then cDNA was combined with ready-to-use RT2 SYBR Green qPCR Master Mix (PA-012, SuperArray Bioscience) in a 96-

well format plate according to the manufacturer's instructions. The qPCR was performed using real-time PCR (7900HT 96-well block, Applied Biosystems). The thermocycler parameters were 95°C for 10 minutes, 40 cycles of 95°C for 15 seconds, and 60°C for one minute. Each sample was used to quantify transcripts specific for the genes modulated as a result of the intracellular signaling pathways engaged and countered by each virus during the infection of the cells. Gene expression of virus-infected cells was compared with mock infected cells at each time point. Relative changes in gene expression were calculated using the Ct (cycle threshold) method. The thresholds and baseline used were the same across all RT-PCR array runs in the same analysis. The Ct values greater than 35 or "not detected" were considered as negative. An average of the number of cycles of the two housekeeping genes, GAPDH (glyceraldehyde-3-phosphate dehydrogenase) and ACTB (actin- $\beta$ ), were used to normalize the expression between samples. The fold-changes in gene expression between virus and mock-infected RNA samples (for pair-wise comparisons) were calculated using the  $\Delta\Delta C_t$  method in PCR Array Data Analysis Web Software portal (SuperArray Bioscience) and transferred into Microsoft Excel format. Expression data was presented as actual fold-change in gene expression. If the fold-change in gene expression was greater than 1, the result was reported as an x-fold up-regulation. If the fold-change was less than 1, then the negative inverse of the result was reported as x-fold down-regulation.

## RESULTS

Cell biosensors analyzed by FTIR at different time points following exposure to each different virus or mock cell lysates produced spectra that could be differentiated by absorption intensity differences at specific wavenumbers. Vero cells were used as the biosensors for detection of HSV-1, Adenovirus, and Coxsackie virus B3, three human pathogenic viruses that represent double-stranded DNA viruses and a positive single strand RNA virus. Each time point was analyzed to determine the earliest time point at which infected cells could be differentiated from uninfected cells and the earliest time point at which each virus could be identified from other viruses. These studies were focused on HSV-1, Coxsackie virus, Adenovirus, and mock infected cells to establish the validity of this unique pathogen detection system.

In order to demonstrate the temporal changes that can be seen during the course of a virus infection, cells were infected with Coxsackie virus at a multiplicity of infection (MOI) of 10, and at selected time points, cells were prepared as described in Materials and Methods. FTIR absorbance spectra were collected from dried cell suspensions in the 1500-800  $\text{cm}^{-1}$  spectral region. Initially, to find the earliest time point at which virus infection could be identified, the spectra were measured for each cell suspension at two, four, six, eight, 12, and 24 hours post infection. By 10 independent repeating experiments under the same conditions, our results showed that observable changes in the IR spectra following virus infection occur at six hours post infection. By eight hours post infection changes in both band positions and band intensities were observed. Furthermore, two small bands at 1153 and 917  $\text{cm}^{-1}$  were shifted up 16 and 8  $\text{cm}^{-1}$  to 1169 and 925  $\text{cm}^{-1}$ , respectively. A dip at 1068  $\text{cm}^{-1}$  decreased with increasing infection time. Peak intensities were increased at 1242  $\text{cm}^{-1}$  and 1085  $\text{cm}^{-1}$  as infection time progressed. In addition peak intensity at 970  $\text{cm}^{-1}$  increased at eight hours post infection. Observations with Coxsackie virus infected cell biosensors are shown in Figure 1.

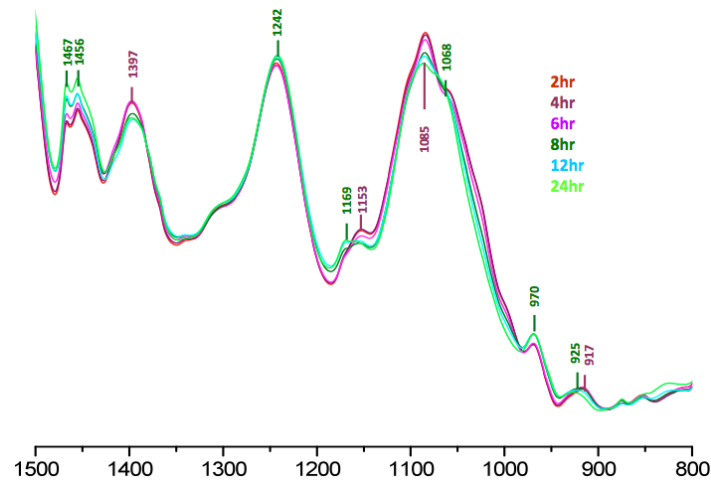


**Figure 1: Averaged IR absorption spectra in the 1500-800  $\text{cm}^{-1}$  region from 10 independent experiments using Coxsackie virus infected cells.** Cells were infected with a multiplicity of infection of 10 at 2 (red), 4 (purple), 6 (magenta), 8 (olive), 12 (blue), and 24 (green) hours post infection. All spectra were vector normalized. The y-axis represents relative absorption intensities. The graph shows obvious spectral changes in band positions and intensities from virus infection.

To determine the earliest time point at which we could see evidence of biosensor signals indicative of specific virus exposures, we infected cells as described and collected spectral data for analysis. Results indicated that six hours following a virus encounter with a cell was sufficient time to discriminate HSV-1 and Coxsackie virus from mock infected cell biosensors. Identification and differentiation of adenovirus has proved to be more challenging, however, biosensors infected with adenovirus can be differentiated from other virus-infected biosensors. Identification and differentiation of adenovirus proved to be more challenging.

To train the designed neural network, we identified the mean values of average standard absorbance at specific band numbers for cells that were infected with HSV-1, adenovirus, or mock infected. These are shown in Figure 2. The bands that were selected at different time points to discriminate which virus infected the cells were  $1086 \text{ cm}^{-1}$  at 2, 4, and 6 hours.  $1301 \text{ cm}^{-1}$  at 2, 4, and 6 hours,  $1301 \text{ cm}^{-1}$  at 6 minus 2 hours, and  $1086 \text{ cm}^{-1}$  minus  $1301 \text{ cm}^{-1}$  at 2, 4, and 6 hours. Discrimination of cells treated with uninfected cell lysates from adenovirus infected lysates failed.

We also developed a partial least squares (PLSR) regression model, using difference spectra (Mock – Mock, Cox – Mock and HSV - Mock) at 6 hours post exposure. For multinomial classification, the PLSR model selected discriminators at 971, 975, 979, 1172, 1222, 1280, 1284, 1287, 1291, 1295, 1299, 1303, 1307 and  $1388 \text{ cm}^{-1}$  and calculated a single predicted value. Figure 3 shows the distribution of the predicted value of the PLSR model for the difference spectra of cells treated with mock infected lysates, Coxsackie virus, and HSV 1. The sensitivity of the PLSR model was 85%, 85 %, and 90% for mock infected lysates, Coxsackie virus and HSV 1, respectively. We observed even better results with binomial classification. The PLSR is similar to multiple linear regression analyses, but permits the analysis of data sets that have more variables than observations.

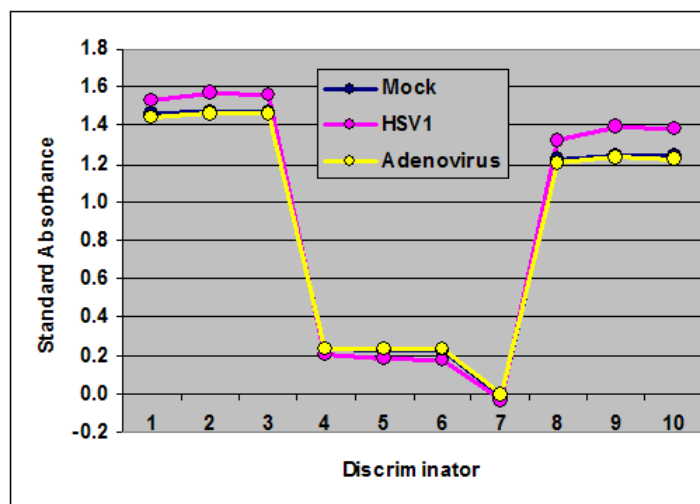


**Figure 2: Mean values of average standard absorbance for the Mock, HSV1 and Adenovirus datasets.** The discriminators from left to right are: (1, 2, 3)  $1086\text{ cm}^{-1}$  at 2, 4 and 6 hours respectively, (4, 5, 6)  $1301\text{ cm}^{-1}$  at 2, 4 and 6 hours respectively, (7)  $1301\text{ cm}^{-1}$  at 6 minus 2 hours, (8, 9, 10)  $1806\text{ cm}^{-1}$  minus  $1301\text{ cm}^{-1}$  at 2, 4 and 6 hours respectively. The network was trained in 10,000 iterations and discriminated HSV1 infection from both Mock and Adenovirus infection with an accuracy of  $28/30 = 0.933$  (95% CI: 0.774 to 0.991) in both the training and test sets. The network failed to discriminate Adenovirus from Mock infection.

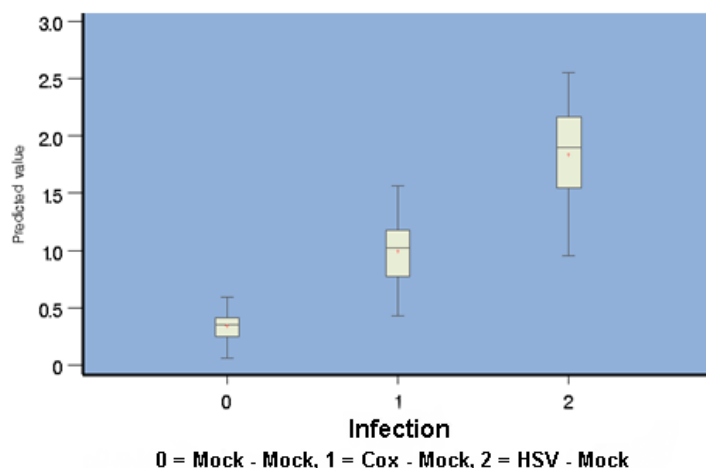


**Figure 3: Box-plot for Mock, HSV1 and Coxsackie infected cells.** The graph shows the distribution of the output of the partial least squares regression (PLSR) model for Mock (0), Coxsackie virus (2) and HSV1 (3) infected cells. The cutoff values were set at Mock:  $<0.1$ , Cox:  $\geq 0.1$  and  $\leq 1.0$  and HSV1:  $> 1.0$ .

### Identification of Molecular Events in Cell Biosensors Following Exposure to Different Viruses

To identify the molecular events in the cells following exposure to virus or mock infected cells at different time points, we identified the cytoplasmic adapter molecules that were phosphorylated. Phosphorylation is one of the major and most frequent modifications induced when homeostasis is disrupted. Cell adapter

molecules are recruited in response to specific insults, e.g., virus infection, bacterial infections, or cancer. Phosphorylation of adapter molecules as they are recruited to complexes that form in a cascade manner, lead to the expression of genes that encode the innate defense components. As countermeasures to this process, viral proteins inhibit those defenses. We hypothesize that by analyzing the pathways that are induced and finding where these are interrupted, the identity of the virus can be revealed. Knowledge of these pathways can help focus FTIR analysis on spectral regions associated with the pathway activities and alterations caused by each specific virus. In these studies, we identified early activation of cytokine and chemokine genes in Coxsackie virus infected cells. Nineteen inflammatory genes in the cell biosensors were induced at 2 hours post Coxsackie virus exposure, whereas biosensors exposed to HSV-1 showed a significant time shift of inflammatory gene induction, reaching a maximum after 8 to 12 hours post infection. The subsets of early-induced genes were also different, as the major distinct molecular markers of Coxsackie virus exposed cells were IL-8, CXCL6, and CCL20 with increased expression at 2 to 4 hours following infection. In contrast, HSV-1 infected cells activated a broader group of genes, including CXCL9, CXCL5, CXCL11, TNF $\alpha$ , LTA, IL9R, CCR4, CCL5, and IL1F6 at 4 to 8 hours post virus infection. The TNF $\alpha$  genes were activated to a greater extent in HSV-1 exposed cells, while IL-8 gene expression exceeded that of TNF $\alpha$  in Coxsackie virus infected cells. Additionally, we observed that HSV-1 up-regulated chemokine receptor gene expression significantly when compared to Coxsackie virus, which down-regulated these genes. In contrast to HSV-1 and Coxsackie virus, adenovirus virus exhibited inflammatory-related gene expression, only detectable after 24 hours following exposure of cells. Table 1 shows the representative relative regulation of each gene involved in cell antiviral responses on the arrays.

**Table 1: Genes up- and down-regulated to a higher level in virus-infected than in mock-infected Vero cells at 2 h post infection.** The red and green arrows mark the up-regulated and down-regulated genes respectively in infected cells. The dashes show the genes with RNA expression values, which did not meet the four-fold change threshold. If unidirectional four-fold changes were observed in 5 out of 5 observations and no changes of less than four-fold were observed in any observations, the 95% confidence interval on the probability of a four-fold threshold difference in expression when compared to mock-infected controls.

Gene symbol	CX 2h	HSV-1 2h	Ad5 2h
CCL2	↑	-	-
CCL20	↑	-	-
CCL23	↑	-	-
CCL24	↑	-	-
CCL7	↑	-	-
CD40LG	↑	-	-
CSF2	↑	↑	-
CXCL1	↑	-	-
CXCL2	↑	-	-
CXCL3	↑	-	-
CXCL6	↑	-	-
EGR1	-	↑	-
FASLG	-	-	↓
FOS	↑	↑	-
IL10	↑	↑	-
IL17C	-	↑	-
IL1F9	↑	-	-
IL5	↓	↓	-
IL8	↑	-	-
IL9R	-	↑	-
LTB	↑	-	-
NFKBIA	↑	-	-
TLR9	-	↑	-
TNF	↑	↑	-

Representative analyses from cells exposed to HSV-1 and Coxsackie viruses are shown in Figure 4 to illustrate the temporal differences in IL-8 and TNF $\alpha$  expression.

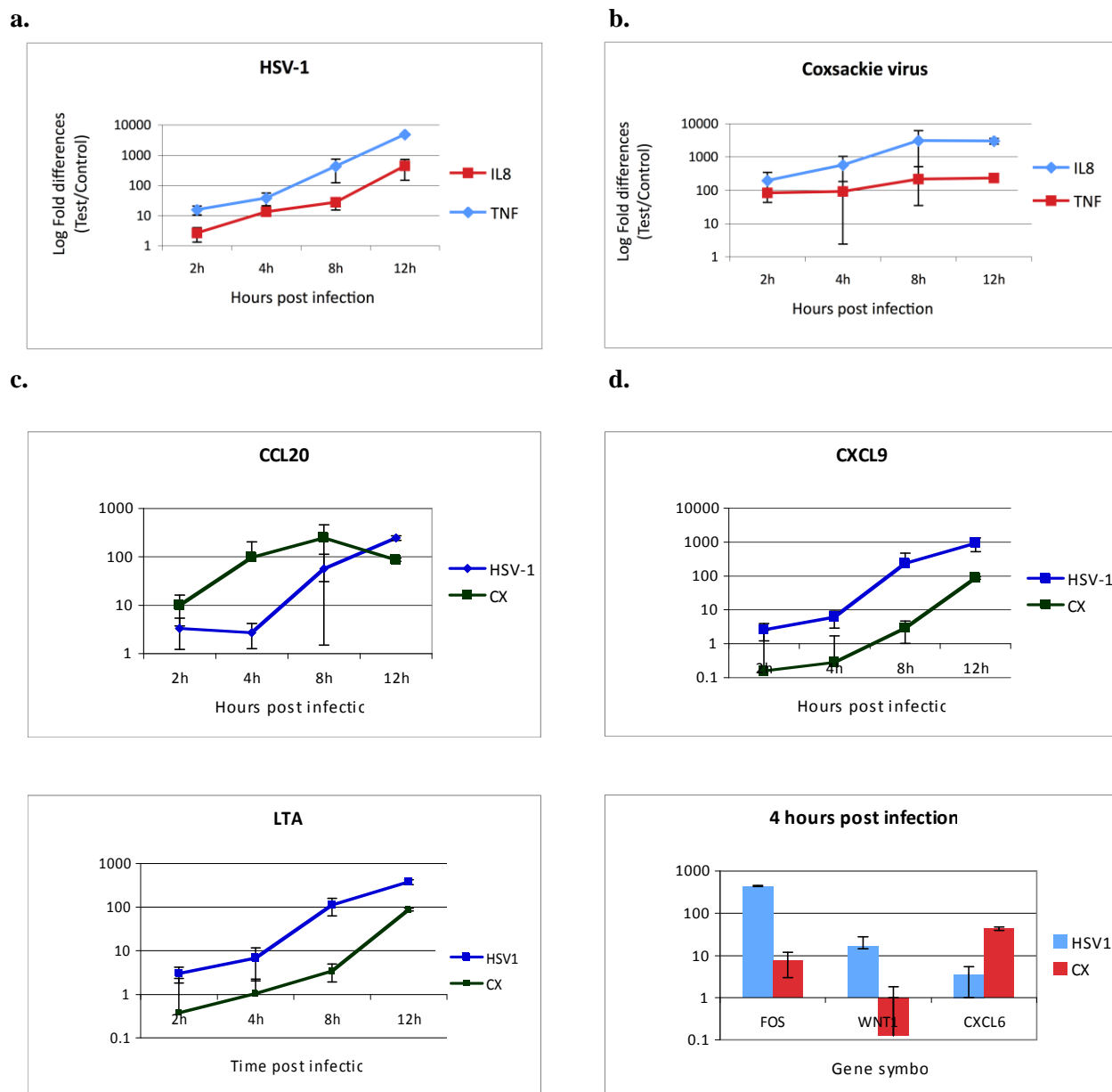


**Figure 4: Kinetics of IL-8 and TNF gene expressions in HSV-1 (a) and Coxsackie (CX) infected cells.**

HSV-1 (a) and coxsackie virus (b) triggered significant transient upregulation of TNF $\alpha$ , and IL8 genes, however HSV-1 delayed IL8 mRNA expression. The IL8 transcript level increased in HSV-1 infected cells after 4 h post infection. The IL8 gene response prevailed over TNF-alpha responses during coxsackie virus infection, while TNF-alpha gene activation dominated that of IL8 during HSV-1 infection. These experiments represent data from (4) independent experiments. (c) Fold-regulation comparative changes between HSV-1 and Coxsackie when measuring chemokines CCL20, CXCL9, CXCL6, cytokine LTA, transcription factor FOS, and WNT1 genes expression. Each data point on the graph is the mean of gene fold-change regulation from at least three independent experiments. Error bars indicate standard deviations.

Analysis of the molecular markers IL-8, TNF $\alpha$ , CCL20, CXCL9, CXCL6, LTA and WNT1 can be used as an example of the different time points at which each virus modulates the cell response to infection. By comparative analysis of fold-change, time, cytokines, and chemokines, these two viruses can be differentiated within 2 to 6 hours after cells were exposed to each. Together, these data demonstrate that pathways that drive the induction of specific genes in infected biosensors are different depending on the virus. Induction patterns as well as temporal differences in some similar pathways can be used to discriminate between cells infected with each virus. The adaptor molecules that drive the transcription of each of the gene sets described will be further studied in order to focus on these as potential correlates of spectral changes over time following infection relative to each virus. Induction of these genes is preceded by cytoplasmic adaptor molecule recruitment with each adaptor being phosphorylated or dephosphorylated to activate the cascade of events leading to the regulation of transcription of cell defense molecules, e.g., cytokines and chemokines.

## **DISCUSSION**

FTIR spectra have been used previously to identify cells at different stages in the cell cycle [6,7] and to identify virus in cells [8,9,10,11] but only after 48-72 hours post infection. In this study, we hypothesized that virus infected cells could be identified within hours post infection by analysis of FTIR spectral patterns. Spectral analysis has been used to identify perturbations in cells [6,12], thus we hypothesized that spectral analysis of cells at early time points post infection could be used to identify the infecting virus. We selected a cell type, Vero cells, that was permissive to the widest number of viruses due to the absence of interferon genes that otherwise make many cell types resistant to virus infections. Since early innate defenses are highly conserved in mammalian cells, however, would not all cells respond similarly? In fact, these defenses are highly conserved, however each virus has selected for traits that have co-evolved with the virus and host in such a manner that the virus and host have a series of orchestrated interactions that result from the virus disruption of host defenses and host countermeasures to circumvent cell death [13,14,15]. Even when similar mechanisms of virus:host interactions exist, temporal differences in these macromolecular interactions exist as shown in this study. Cells, in fact, are perhaps the most sensitive detectors of pathogens and spectral analysis of cells under attack reveal that infected cells can be identified, as well as the virus that is causing the infection, all within hours after the host:virus encounter occurs.

This work reveals for the first time that analysis of FTIR spectra from cells can be used to identify viruses within 2 to 6 hours post infection and that viruses can be differentiated based upon the spectra from chemical changes within cells. The macro molecular events that correlate with cell spectra are not currently known, but validation of differences in molecular activities of cells infected with different viruses is presented here to demonstrate that molecular events in the infected cell confirm that each of these viruses modulate the cell differently and uniquely. Identification of unknown viruses at this early stage of infection using this novel diagnostic approach has the potential to revolutionize the identification of infectious diseases. Clinical providers can use this technology for rapid pathogen identification to implement specific therapies within hours after seeing patients suffering from infections. Similarly, critical supply sources, e.g., water, soil, food supplies can be monitored for pathogen contamination. Currently available technologies require days to weeks to identify infectious agents, while this technology promises rapid identification of pathogens within hours following exposure of cells to pathogen contaminated samples.

## **ACKNOWLEDGMENTS**

Special appreciation is extended to Nina Beato, Project Manager who maintains all data collected by individual investigators. This work was funded by U.S. Army Medical Research Award [W81XWH-06-1-0795](#).

## REFERENCES

- [1] Juckem LK, Boehme KW, Feire AL, Compton T (2008) Differential initiation of innate immune responses induced by human cytomegalovirus entry into fibroblast cells. *J Immunol* 180: 4965-4977.
- [2] Vercammen E, Staal J, Beyaert R (2008) Sensing of viral infection and activation of innate immunity by toll-like receptor 3. *Clin Microbiol Rev* 21: 13-25.
- [3] Nociari M, Ocheretina O, Schoggins JW, Falck-Pedersen E (2007) Sensing infection by adenovirus: Toll-like receptor-independent viral DNA recognition signals activation of the interferon regulatory factor 3 master regulator. *J Virol* 81: 4145-4157.
- [4] Hastings G, Wang R, Krug P, Katz D, Hilliard J (2008) Infrared microscopy for the study of biological cell monolayers. I. Spectral effects of acetone and formalin fixation. *Biopolymers* 89: 921-930.
- [5] Hastings G, Krug P, Wang R, Guo J, Lamichhane HP, et al. (2009) Viral infection of cells in culture detected using infrared microscopy. *Analyst* 134: 1462-1471.
- [6] Mourant JR, Yamada YR, Carpenter S, Dominique LR, Freyer JP (2003) FTIR spectroscopy demonstrates biochemical differences in mammalian cell cultures at different growth stages. *Biophys J* 85: 1938-1947.
- [7] Liu R, Tang W, Kang Y, Si M (2009) Studies on best dose of X-ray for Hep-2 cells by using FTIR, UV-vis absorption spectroscopy and flow cytometry. *Spectrochim Acta A Mol Biomol Spectrosc* 73: 601-607.
- [8] Erukhimovitch V, Talyshinsky M, Souprun Y, Huleihel M (2005) FTIR microscopy detection of cells infected with viruses. *Methods Mol Biol* 292: 161-172.
- [9] Erukhimovitch V, Mukmanov I, Talyshinsky M, Souprun Y, Huleihel M (2004) The use of FTIR microscopy for evaluation of herpes viruses infection development kinetics. *Spectrochim Acta A Mol Biomol Spectrosc* 60: 2355-2361.
- [10] Huleihel M, Talyshinsky M, Souprun Y, Erukhimovitch V (2003) Spectroscopic evaluation of the effect of a red microalgal polysaccharide on herpes-infected Vero cells. *Appl Spectrosc* 57: 390-395.
- [11] Salman A, Erukhimovitch V, Talyshinsky M, Huleihil M, Huleihel M (2002) FTIR spectroscopic method for detection of cells infected with herpes viruses. *Biopolymers* 67: 406-412.
- [12] Andrus PG (2006) Cancer monitoring by FTIR spectroscopy. *Technol Cancer Res Treat* 5: 157-167.
- [13] Hale BG, Kerry PS, Jackson D, Precious BL, Gray A, et al. (2010) Structural insights into phosphoinositide 3-kinase activation by the influenza A virus NS1 protein. *Proc Natl Acad Sci U S A* 107: 1954-1959.
- [14] Doehle BP, Hladik F, McNevin JP, McElrath MJ, Gale M, Jr. (2009) Human immunodeficiency virus type 1 mediates global disruption of innate antiviral signaling and immune defenses within infected cells. *J Virol* 83: 10395-10405.



- [15] Foy E, Li K, Sumpter R, Jr., Loo YM, Johnson CL, et al. (2005) Control of antiviral defenses through hepatitis C virus disruption of retinoic acid-inducible gene-I signaling. *Proc Natl Acad Sci U S A* 102: 2986-2991.